Chemical Proteomics-Based Drug Design: Target and Antitarget Fishing with a Catechol−Rhodanine Privileged Scaffold for NAD(P)(H) Binding Proteins

Xia Ge,[†] Bassam Wakim,[‡] and Daniel S. Sem*,[†]

Department of Chemistry, Chemical Proteomics Facility at Marquette, P.O. Box 1881, Marquette University, Milwaukee, Wisconsin 53201, and Medical College of Wisconsin, Milwaukee, Wisconsin 53226

Received March 3, 2008

Drugs typically exert their desired and undesired biological effects by virtue of binding interactions with protein target(s) and antitarget(s), respectively. Strategies are therefore needed to efficiently manipulate and monitor cross-target binding profiles (e.g., imatinib and isoniazid) as an integrated part of the drug design process. Herein we present such a strategy, which reverses the target → lead rational drug design paradigm. Enabling this approach is a catechol−rhodanine *privileged scaffold* for dehydrogenases, which is easily tuned for affinity and specificity toward desired targets. This scaffold crosses bacterial (*E. coli*) cell walls, and proteome-wide studies demonstrate it does indeed bind to and identify NAD(P)(H)-binding proteins that are potential drug targets in *Mycobacterium tuberculosis* and antitargets (or targets) in human liver. This approach to drug discovery addresses key difficulties earlier in the process by only pursuing targets for which a chemical lead and optimization strategy are available, to permit rapid tuning of target/antitarget binding profiles.

The drug discovery process is costly and often inefficient.[1] Genomics and proteomics advances have presented the promise of improving efficiency, but this has largely translated into the identification of new drug targets, not new drugs. What is needed is a better coupling of the chemistry of drug design to advances in genomics and proteomics. To partially address this, chemical genetic approaches have been developed,[2,3] where enzyme inhibitors are used to knock out protein function. One advantage of chemical genetics over traditional genetics is that besides providing phenotypic data in the context of a whole organism, it yields an inhibitor for subsequent optimization in the drug discovery process. Still, this process is problematic in two ways: (a) one cannot be certain that the inhibitor binds only to the intended target, and (b) it is highly inefficient because new inhibitors must be designed for each new target of interest. The first question is relevant because binding to other proteins (antitargets) can lead to toxic side effects. Further complicating matters, in other cases such as imatinib[4–6] (4-[(4-methyl-1-piperazinyl)methyl]-*N*-[4-methyl-3-[[4-(3-pyridinyl)-2-pyrimidinyl]amino]phenyl]benzamide methanesulfonate) and isoniazid,[7] off-target binding is actually thought to contribute to drug efficacy, thereby calling into question the one-target/one-drug dogma that serves as the foundation for rational drug design. The second question is relevant because the process of designing potent inhibitors that are acceptable drug leads can take years and varies in difficulty from protein to protein, being nearly impossible for some protein targets, leading to the notion of "druggable" protein targets.[8,9] There is a vital need to identify "druggable targets" (those for which potent and selective inhibitors can be designed) as early in the drug discovery process as possible. To address this second concern, compounds can be designed based on "privileged scaffolds",[10–13] which are druglike[14,15] molecular structures that provide baseline affinity for a whole protein family. These scaffolds then serve as starting points for optimization against specific protein targets of interest in the family, usually by building a focused combinatorial library off of the scaffold. To this end, privileged scaffolds have been reported for kinases,[16] proteases,[17,18] and GPCRs.[19,20] We have recently reported the first privileged scaffold for NAD(P)(H)-binding proteins,[21] based on a catechol−rhodanine ring system. Proteins in this family include the oxidoreductases (aka dehydrogenases), with drug targets such as HMG-CoA reductase (statin drugs), steroid-5α-reductase (finasteride), aldose reductase (diabetes), and a large number of infectious disease targets,[22,23] including enoyl CoA reductase, deoxyxylulose-5-phosphate reductoisomerase (DOXPR), and dihydrodipicolinate reductase (DHPR[a]); this family even includes enzymes other than oxidoreductases, such as sirtuins, ADP-ribosylating enzymes, and ligases. The catechol−rhodanine privileged scaffold has served as a template for building biligand libraries, where the ligand attached to the scaffold is situated in the substrate pocket, thereby giving specificity to a particular enzyme in the family (Figure 1). It has been used to generate multiple potent ($K_d \leq$ 200 nM) and selective inhibitors for dehydrogenases, including DHPR and DOXPR,[21] with affinity and selectivity readily tuned by varying the fragment attached to the scaffold.

Despite the power of this scaffold, it has never been properly verified as being specific for NAD(P)(H)-binding enzymes in a proteome-wide manner. This is because a strategy was not available to assess cross-reactivity (off-target binding) with other family members, in the context of a whole proteome, whether for the catechol−rhodanine scaffold itself or for biligand drug leads constructed from it, for specific targets. This gets to the

* To whom correspondence should be addressed. Phone: 414-288-7859. Fax: 414-288-7066. E-mail: Daniel.Sem@marquette.edu.
[†] Marquette University.
[‡] Medical College of Wisconsin.

[a] Abbreviations: ADME, absorption, distribution, metabolism, and excretion; CRAA, catechol−rhodanine acetic acid; DCC, *N,N′*-dicyclohexylcarbodiimide; DCU, dicyclohexylurea; DHPR, dihydrodipicolinate reductase; DMAP, 4-(dimethylamino)pyridine; ESI, electrospray ionization; HPLC, high performance liquid chromatography; IPTG, Iisopropyl β-D-1-thiogalactopyranoside; LC-MS, Liquid Chromatography−Mass Spectrometry; LTQ, Linear Trap Quadrupole; NHS, N-hydroxysuccinimide ester; NMR-SOLVE, structurally oriented library valency engineering; PAGE, polyacrylamide gel electrophoresis; PBS, phosphate buffered saline; SDS, sodium dodecyl sulfate; TB, tuberculosis; Tris, tris(hydroxymethyl)aminomethane; TEMED, tetramethylethylenediamine.

10.1021/jm8002284 CCC: $40.75
Published on Web 07/11/2008

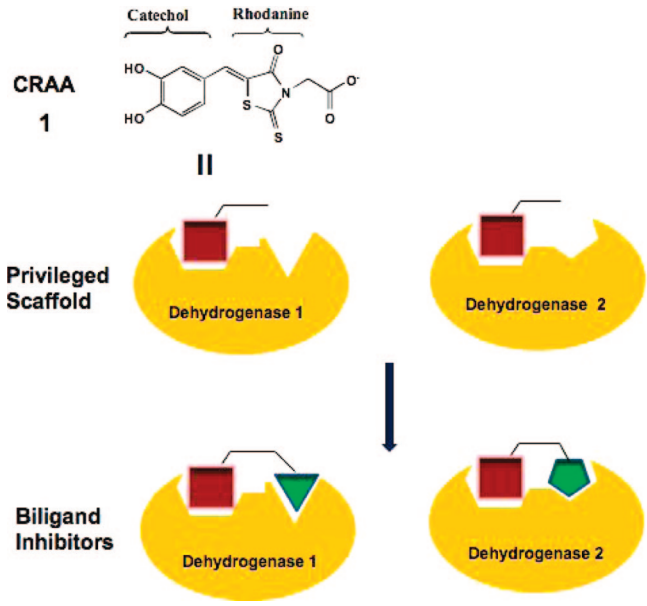

Figure 1. Catechol−rhodanine privileged scaffold (CRAA, **1**) and its use in creating biligand inhibitors with high affinity and specificity for specific dehydrogenase targets.

first concern mentioned above. Recent advances in chemical proteomics[6,24,25] now permit proteome-wide binding studies of the scaffold (and later, of biligands) by covalently attaching scaffold to a resin, binding all protein family members in a proteome sample, then eluting with free scaffold (or biligand) and identifying proteins with tandem MS. Such a strategy was recently used to assess binding profiles for currently prescribed drugs, such as imatinib[4–6] and isoniazid.[7] Both of these drugs were thought to bind tightly to a single target, and it was later discovered that their biological efficacy might actually be due to binding to multiple targets. The strategy and tools presented in this paper would now permit the assessment and optimization of cross-target binding profiles (target/antitarget) across a proteome as an integral part of the drug design process; in this manner, binding profiles could be correlated with biological efficacy up front in a rational manner rather than relying on serendipitous and unknown off-target effects.

The strategy proposed herein depends crucially on the availability of a privileged scaffold that binds to a protein family (dehydrogenases, in this case) and that has been designed in such a way that it can be quickly modified to produce potent inhibitors for a given family member (building biligands, in this case). The latter has already been verified[21] for the privileged scaffold that is the topic of this paper, which is based on the catechol−rhodanine acetic acid **1** (CRAA) shown in Figure 1. But is this scaffold a viable starting point for drug discovery? While the thiazolidine ring (rhodanine is a type of thiazolidine) has been reported by Poupaert et al.[26] as a frequently occurring heterocyclic motif in anti-inflammatory, antipsychotic, and anticonvulsant drugs, the rhodanine ring is less common. But it does occur in drugs such as epalrestat ((2-[(5*Z*)-5-[(*E*)-3-cyclohexyl-2-methylprop-2-enylidene]-4-oxo-2-thioxo-3-thiazolidinyl]acetic acid)), a potent inhibitor of aldose reductase (AR), and has been shown to have no significant toxicity in recent clinical trials.[27,28] The catechol group, though present in a number of plant-derived natural products, can have toxicity in some cases when it is oxidized to an *o*-quinone, which can then alkylate cellular macromolecules or generate reactive oxygen species.[29,30] As such, **1** does seem to be a viable scaffold upon which to build drug leads, using the strategies described herein, with the caveat that the *o*-catechol may need to be replaced if there is any toxicity.

The chemical proteomic strategy proposed herein also relies on attaching a dehydrogenase-specific ligand to a resin, using that affinity column with subsequent digestion of the eluted proteins, and subjecting the tryptic peptides to electrospray LC/MS followed by searching the MS/MS data against an appropriate subset of the Uniprot database to identify all (reasonably abundant) proteins in a proteome that bind the ligand. While affinity purification using native cofactor has been applied to dehydrogenases for over 30 years,[31–33] it has never been coupled to tandem MS to probe binding profiles for a dehydrogenase-targeted privileged scaffold. And more broadly, although there is emerging interest in using affinity chromatography coupled to mass spectrometry to probe protein−ligand interactions across a proteome,[34] there is a need for more efficient coupling of this assay methodology earlier in the drug design process, using the chemical leverage provided by privileged scaffolds to create an integrated drug discovery approach that blends (a) a broad assessment of target/antitarget binding profiles, (b) a pragmatic selection of druggable targets, and (c) an efficient chemical strategy for tuning target/antitarget affinity. This paper presents a foundation for such a strategy, applied using the first such privileged scaffold for NAD(P)(H) binding proteins.

Results

2 (NHS-CRAA) Uptake into *E. coli* Cells and Labeling of DHPR. To assess whether **1** (CRAA) can make it across bacterial cell walls and therefore whether **1** is a viable scaffold for anti-infective drug design efforts, experiments were performed to determine if its *N*-hydroxysuccinimide ester, **2** (NHS-CRAA, Figure 2), could enter *E. coli* and label intracellular DHPR (dihydrodipicolinate reductase). DHPR is an anti-infective drug target and is known to bind the CRAA scaffold (**1**).[21] The NHS-CRAA active ester (**2**)[35] was synthesized as in Figure 2. The NHS (*N*-hydroxysuccinimide) group reacts with amines, and since it is attached to the linker position of **1** (where the acetic acid chain is attached), it should reside at the interface of the NADH and substrate binding sites[21] (Figure 1), near lysine 163[36] (see Supporting Information Figure S1). Indeed, DHPR is labeled with the NHS-CRAA (**2**) active ester, based on imaging of an SDS−PAGE gel of labeled protein (Supporting Information Figure S1). Labeling is partially blocked by NADH (Figure S2), indicating that the NHS-CRAA (**2**) probe is in fact binding and labeling (at least partially) in the active site of DHPR. Next, to explore whether cell wall penetration occurs, uptake of **2** was measured into *E. coli* that was expressing *E. coli* DHPR. Since we have recently shown that the CRAA scaffold (**1**) is bifunctional, in that it is itself weakly fluorescent,[33] protein labeling could be monitored by fluorescence imaging of SDS−PAGE gels of crude cell extracts. In-cell studies were performed by overexpressing DHPR in *E. coli*, then exposing intact cells to the NHS-CRAA probe (**2**), washing and lysing cells, and then running an SDS−PAGE gel to see if the probe was able to covalently label the DHPR (Figure 3a). Any NHS-CRAA probe (**2**) that was nonspecifically associated with the cells was quenched by treatment with 100 mM Tris before lysis. Gels show that significant labeling of the DHPR did occur within the intact *E. coli* cells (Figure 3b), indicating that scaffold can cross the cell wall in order to gain access to DHPR. That there is more labeling in cells expressing DHPR is evident based on the more intense color for cells expressing DHPR (Figure 3c) and on fluorescence images of the cells (Figure 4a).

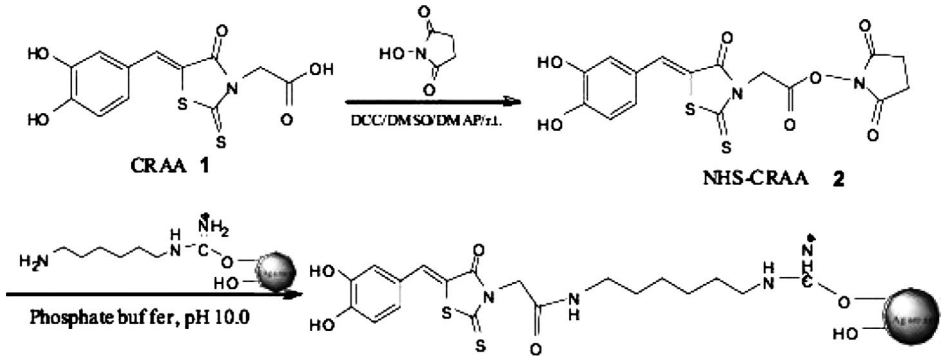

Figure 2. Synthesis of the NHS-CRAA active ester (**2**) and CRAA aminohexylagarose matrix.

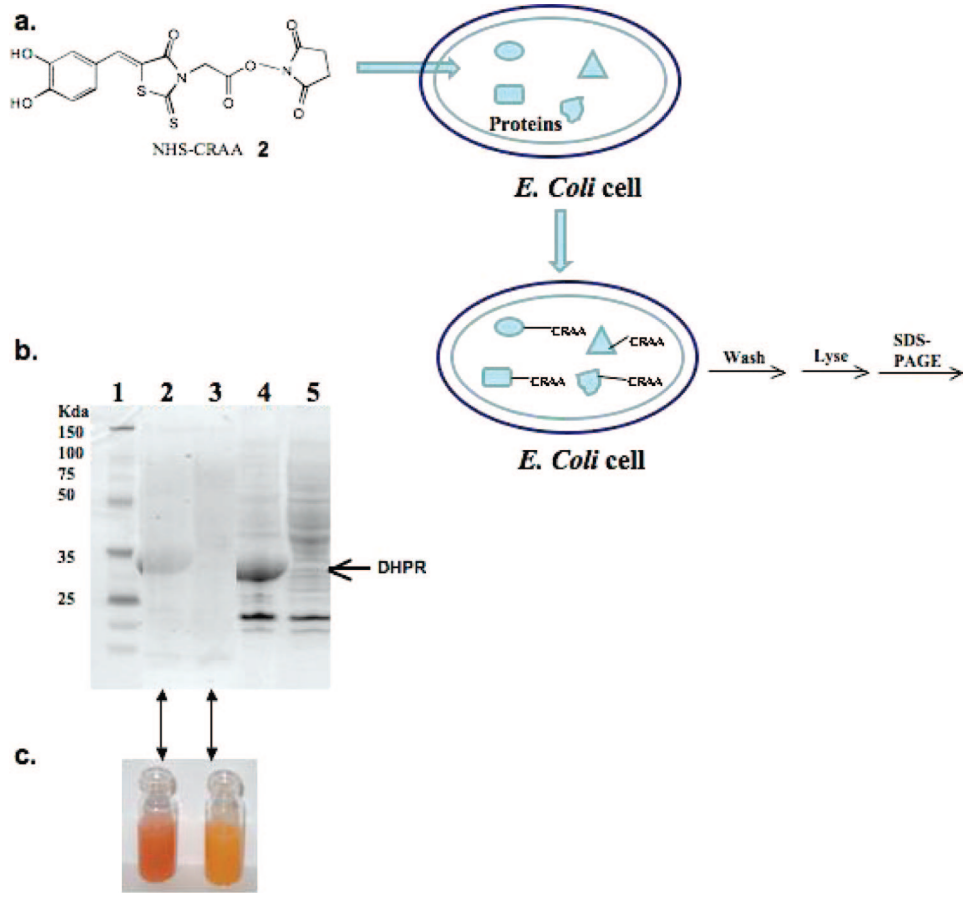

Figure 3. (a) *E. coli* uptake study. Cartoon representation of the uptake study demonstrating that NHS-CRAA ester (**2**) can cross the *E. coli* cell wall to react with overexpressed DHPR and other intracellular proteins. (b) SDS−PAGE analysis of the crude cell lysate from the experiment in part a. Lane 1: protein marker. Lanes 2 and 4: lysate of cells with DHPR present (+IPTG). Lanes 3 and 5: lysate of cells without DHPR present (−IPTG). Lanes 2 and 3 were fluorescently scanned using a Kodak Image Station. Lanes 4 and 5 were scanned with a CanonScan D1250U2F document scanner after Coomassie blue staining, used with the same Gel. (c) Vials of *E. coli* cells just prior to lysis, showing the CRAA-associated color change in the cells containing overexpressed DHPR (left) relative to those without DHPR (right).

CRAA (1) Affinity Chromatography and Nanospray-LC/MS/MS. Our proteome fishing studies (Figure 5) require a resin with a privileged scaffold, in this case **1**, covalently attached. The NHS-CRAA (**2**) active ester (Figure 2) was used to prepare this affinity resin to permit purification of dehydrogenase (NAD(P)(H)-binding protein) subproteomes from protein mixtures. Crude cell lysates from *E. coli* and *M. tuberculosis* were both loaded onto the affinity column, and proteins were eluted using free CRAA (**1**) probe, as shown in Figure 5. SDS−PAGE analysis of both microbial samples showed very similar patterns (Figure 6a), although analysis of proteins that were identified from *M. tuberculosis* (vide infra, Table 2) indicates that some proteins have no *E. coli* homologues, and for those that do, masses differ. So the apparent similarity in gel patterns is more likely due to the prevalence of proteins in these molecular weight ranges in both microbes. As with the microbial samples, human liver proteins were loaded onto the affinity resin and eluted with **1** (Supporting Information and Figure 6b), to determine the CRAA-binding profile for the liver proteome. It is noteworthy in this gel, which shows wash and elution fractions, that proteins are specifically eluted by free **1**.

For both human liver and *M. tuberculosis* eluents, nanospray-LC/MS/MS analysis was performed followed by searching the MS/MS data against an appropriate subset of the Uniprot database to determine which CRAA-binding proteins were present in reasonably high abundance. To complement this

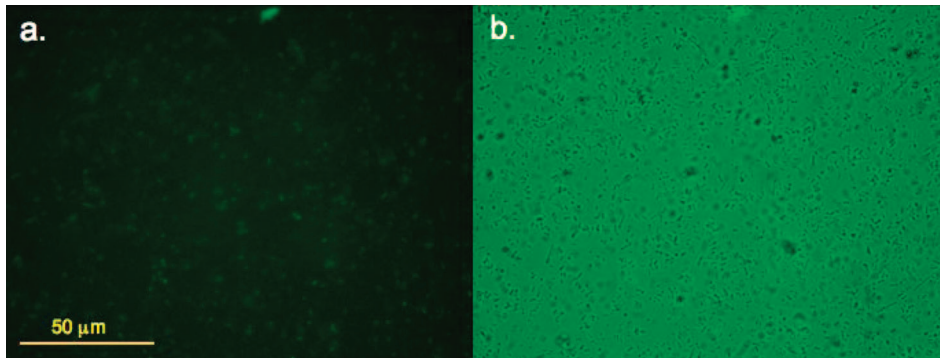

Figure 4. *E. coli* fluorescence labeling: (a) fluorescence and (b) bright field images of *E. coli* cells containing overexpressed DHPR, after incubation with NHS-CRAA (**2**) and subsequent washing with PBS. A 100× objective and 495 nm/520 nm excitation/emission filters were used.

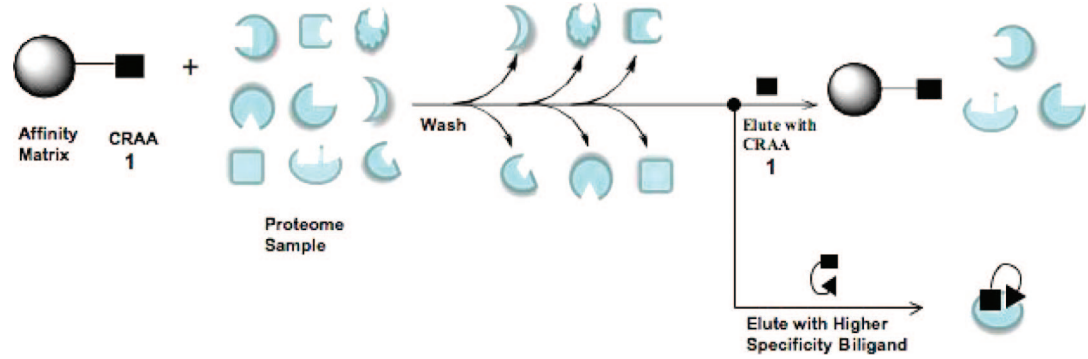

Figure 5. Proteome fishing with a privileged scaffold. Cartoon representation of how the CRAA (**1**) affinity column is used for target fishing in a proteome pool either to initially identify potential targets and antitargets (top branch) or to later characterize the binding profile for a particular biligand drug lead candidate (bottom branch). The top branch also demonstrates how one assesses whether a privileged scaffold really is targeting a gene family (as intended), such as NAD(P)(H) binding proteins.

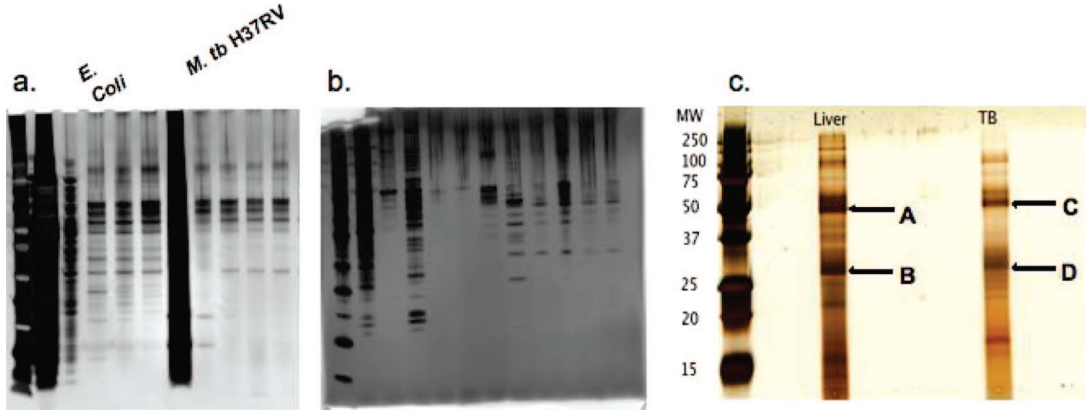

Figure 6. SDS−PAGE analysis of the proteome fishing experiments described in Figure 5. (a) SDS−PAGE analysis of CRAA-captured proteins from *E. coli* and *M. tuberculosis* H37Rv proteomes. Lane 1: protein marker. Lane 2: *E. coli* crude cell lysate. Lane 3: *E. coli* column wash. Lanes 4−6: *E. coli* fractions after elution with free CRAA (**1**). Lane 7: *M. tuberculosis* crude cell lysate. Lane 8: *M. tuberculosis* column wash. Lanes 9−11: *M. tuberculosis* fractions after elution with free CRAA (**1**). (b) SDS−PAGE analysis of CRAA-captured proteins from human liver proteome. Lane 1: Protein marker. Lane 2, crude cell lysate. Lanes 3−5: column wash. Lanes 6−12: fractions after elution with free CRAA (**1**). (c) SDS−PAGE analysis of human liver and *M. tuberculosis* H37Rv protein fractions after CRAA (**1**) affinity column chromatography, showing the protein bands that were cut and extracted for nanospray-LC/MS/MS proteomic analysis. Samples identical to those loaded on the gel were polymerized in a gel piece as described in Methods and subjected to whole proteomic analyses. Labeled bands A−D are referred to in Table 3 (database search results). Gels were silver-stained.

whole proteome (actually subproteome) analysis, CRAA-eluted fractions were also separated using SDS−PAGE, and protein bands at ∼35 and ∼55 kDa (Figure 6c) were in-gel-digested. Then peptides were extracted from the gel and analyzed as above. In both cases, proteins were first digested with trypsin, then zip-tip-cleaned and injected into an LC−MS system (LTQ with a linear ion trap from Thermo-Fisher). Whole subproteome analyses are in Table 1 (human liver) and Table 2 (*M. tuberculosis*), while analysis of extracted bands is in Table 3. Complete data sets, even for very low scoring hits, are given in Supporting Information (Figures S8 and S9). Generally, LC/MS data indicate that >50% of these proteins are dehydrogenases or other NAD(P)(H) binding proteins, as expected. Better identifications were obtained from the human liver sample, perhaps because the *M. tuberculosis* sample workup involves irradiation, which may cause some protein damage. In any case,

Table 1. Mass Spectrometry-Based Identification of Proteins Identified in the Target Fishing Study Using the CRAA Affinity Column: Human Liver Proteome[a]

accession number (gi)	annotated function (human)	molecular weight (Da)	coverage (%)	score
6648067	**malate dehydrogenase, mitochondrial precursor**	35 531	52	1557
1346343	keratin, type II cytoskeletal 1	66 018	23	852
113611	fructose-bisphosphate aldolase B (liver-type aldolase)	39 473	24	643
118504	**aldehyde dehydrogenase, mitochondrial precursor**	56 381	28	526
118541	**glutamate dehydrogenase 1, mitochondrial precursor**	61 398	29	523
118495	**retinal dehydrogenase 1 (aldehyde dehydrogenase family 1 member A1)**	54 862	22	377
81175178	keratin, type I cytoskeletal 9 (cytokeratin-9) (CK-9) (keratin-9) (K9)	62 129	30	346
59802911	**10-formyltetrahydrofolate dehydrogenase (aldehyde dehydrogenase family 1 member L1)**	98 829	15	252

[a] Pyridine nucleotide (NAD(P)(H)) binding proteins are indicated in bold. Annotation is directly from the database.

Table 2. Mass Spectrometry-Based Identification of Proteins Identified in the Target Fishing Study Using the CRAA Affinity Column: *M. tuberculosis* Proteome[a]

accession number (gi)	annotated function (*Mycobacterium tuberculosis*)	molecular weight (Da)	coverage (%)	score
81671721	**possible oxidoreductase**[b]	33 220	30	80
54036852	chaperone protein clpB	92 568	15	31
2829534	**riboflavin biosynthesis protein ribD [includes diaminohydroxyphosphoribosylaminopyrimidine deaminase]**	35 366	8	26
1706274	bifunctional enzyme cysN/cysC [includes sulfate adenylyltransferase subunit 1]	67 839	3	20
81671959	**putative uncharacterized protein**[c]	30 296	30	17
81340808	**putative uncharacterized protein**[d]	38 520	16	13

[a] Pyridine nucleotide (NAD(P)(H)) binding proteins are indicated in bold. Annotation is directly from the database. Of the *M. tuberculosis* nucleotide (NAD(P)(H)) binding proteins indicated, two have homologues in *E. coli*: gi81671721 is similar to the *E. coli* protein gi75240619 (M_r = 42 233 g/mol), and gi2829534 is similar to the *E. coli* protein gi75230139 (M_r = 39 456 g/mol). [b] A subsequent NCBI search indicates this protein has homology to coenzyme F420-dependent N5,N10-methylene tetrahydromethanopterin reductase or other flavin-dependent oxidoreductases. [c] A subsequent NCBI search indicates this protein has homology to 17-β-hydroxysteriod dehydrogenase and to hydratase-dehydrogenase-epimerase. It contains the *R*-hydratase-like hot dog fold. Other proteins with this fold include fatty acid synthase beta subunit and MaoC dehydratase. [d] Protein of closest homology with annotated function, based on a BLAST search ($E = 10^{-24}$), is the nitroreductase from *Burkholderia dolosa* (gi:124901246). Enzymes in this family catalyze the NAD(P)H dependent reduction of flavin or nitro compounds using FMN or FAD as cofactor.

several *M. tuberculosis* proteins could be identified with high certainty. Analysis of extracted bands was intended as a check on the whole subproteome analyses, although in general there was lower signal-to-noise (and, as a consequence, scores) for these samples. Still, there is generally good agreement between extracted band data and whole subproteome analysis, especially when scores are higher (>10) and percent coverage of the protein sequence is more complete (≥7%).

Of the highest scoring human liver proteins (Table 1), 5 out of 6 (excluding keratin, a very abundant protein) were dehydrogenases. The top hit, malate dehydrogenase, has more than 50% peptide coverage and a very high score, while glutamate, aldehyde, and retinal dehydrogenases also had high percent coverage (>20%). Binding of **1** to two of these dehydrogenases (glutamate and malate) was subsequently verified experimentally in NMR STD (saturation transfer difference) binding assays (Supporting Information Figure S7). Other dehydrogenases that appear to bind 1, based on lower but still statistically significant scores and percent coverage, include (Supporting Information Figure S8) alcohol dehydrogenases, isocitrate dehydrogenase, α-aminoadipic semialdehyde dehydrogenase (gi116241244), and NADP-dependent leukotriene B4 12-hydroxydehydrogenase (gi23503081). It is noted that for tandem MS analysis of bands at around 55 and 35 kDa, isocitrate/aldehyde and malate dehydrogenases, respectively, are again identified with high certainty, confirming that they do indeed bind to **1**.

As with the liver proteins, *M. tuberculosis* proteins were bound to the CRAA-affinity resin, then eluted with free CRAA (**1**), and fractions were analyzed using electrospray LC/MS/MS. Of the highest scoring (score >13) *M. tuberculosis* proteins (Table 2), there were four possible pyridine nucleotide-binding proteins out of six proteins identified. The other proteins bind ATP, so the CRAA scaffold (**1**) may have some modest affinity for ATP binding sites as well. Interestingly, three of the proteins

Table 3. Mass Spectrometry-Based Identification of Proteins Captured in the Target Fishing Study Using the CRAA Affinity Column: Analysis of Proteins Extracted from Bands[a]

accession number (gi)	annotated function (human)	molecular weight (Da)	coverage (%)	score
	(A) Human Liver Proteins in Band A (45−60 kDa)			
74762137	tubulin β-2A chain[b]	49 906	26	148
21903432	**isocitrate dehydrogenase [NADP] cytoplasmic (cytosolic NADP-isocitrate dehydrogenase)**[b]	46 659	24	84
118504	**aldehyde dehydrogenase, mitochondrial precursor (ALDHclass 2)**[b]	56 381	16	36
55977864	tubulin α-1A chain (tubulin B-α-1) (tubulin α-3 chain) (α-tubulin 3)[b]	50 135	15	19
	(B) Human Liver Proteins in Band B (30−35 kDa)			
6648067	**malate dehydrogenase, mitochondrial precursor**[b]	35 531	7	3

accession number (gi)	annotated function (*Mycobacterium tuberculosis*)	molecular weight (Da)	coverage (%)	score
	(C) *Mycobacterium tuberculosis* Proteins in Band C (50−65 kDa)			
2829534	**riboflavin biosynthesis protein ribD**	35 366	8	4
1706274	bifunctional enzyme cysN/cysC[b]	67 839	3	3
2497387	putative transposase Rv3428c	45 494	2	2
	(D) *Mycobacterium tuberculosis* Proteins in Band D (30−35 kDa)			
81671721	**possible oxidoreductase**[b]	33 220	27	78
81668779	exopolysaccharide phosphotransferase cpsY	60 268	2	7
1706274	bifunctional enzyme cysN/cysC	67 839	3	3
2829534	**riboflavin biosynthesis protein ribD**[b]	35 366	8	3

[a] Pyridine nucleotide (NAD(P)(H)) binding proteins are indicated in bold. [b] Only these proteins have the correct mass for the extracted band(s).

had no annotated function, but a subsequent NCBI search (i.e., updated annotation) and BLAST alignments identified the closest homologues to in fact be NAD(P)(H) binding proteins. This highlights the potential value of CRAA (**1**) target fishing in functional proteomic efforts, by even capturing uncharacterized proteins and providing suggestive data on their cofactor binding preferences, as well as the start of a chemical genetic probe.

Discussion

The methods presented herein were developed to address two of the major roadblocks in drug design projects and in the development of chemical genetic probes (i.e., functional genomics): (a) there is a need to know the binding profile (target, antitarget binding) for a molecule as broadly as possible, whether it is a privileged scaffold that targets many proteins in a gene family or a highly specific drug lead intended for one protein, and (b) there is a desperate need to speed up chemistry by including, integral to this process, a strategy for rapid tuning of a binding profile; this is accomplished by using a privileged scaffold that can be rationally modified to target a protein of interest (Figure 1). A central element of this pragmatic approach to drug discovery is to make sure that protein targets are only pursued if a druglike inhibitor is already in hand, which can be rationally modified for higher affinity with minimal effort. This addresses up front the common concern over whether a protein target is "druggable". One additional drug discovery challenge, in the case of anti-infectives, is the formidable barrier of needing to cross the microbial cell wall. The studies presented herein present a strategy to drug discovery that attempts to address all of these problems, with a focus on NAD(P)(H)-binding proteins. The approach relies on the availability of a privileged scaffold that targets a gene family and that is easily modified to achieve higher affinity for a given target. We have previously described such a probe for NAD(P)(H)-binding proteins,[21] which is shown in Figure 1. The study presented herein extends this work by (a) showing that this scaffold is able to cross bacterial cell walls (Figures 3 and 4), (b) demonstrating that it truly is a privileged scaffold for NAD(P)(H) binding proteins (Tables 1–3) based on proteome-wide profiling (Figures 5 and 6), and (c) identifying potential drug targets (Table 2) and antitargets (Table 1) to be pursued in future drug design efforts, coupled with proteome-wide profiling studies (Figure 5).

With regard to penetrating bacterial cell walls, uptake studies were performed by monitored labeling of intracellular proteins using the CRAA (**1**) privileged scaffold tethered to an amine-reactive reagent. This is effectively an activity-based probe, analogous to those described for other protein families in the field of chemical proteomics[38,39] but not yet reported for NAD(P)(H) binding proteins. The attachment point for the NHS group was chosen to be at the end of the CRAA (**1**) linker, in the position that is normally proximal to or in the substrate site (Figure 1), so it will only label proteins that have an amine in that position. Fortunately (and by design), DHPR has an amine in this position, and so it could be labeled. Incubation of purified DHPR with NHS-CRAA (**2**) does in fact lead to covalent labeling (Supporting Information Figures S1 and S2). Labeling is also observed if intact *E. coli* cells that are overexpressing DHPR are exposed to probe (Figures 3 and 4). This could only happen if the probe can cross the cell wall, providing unambiguous evidence that there is nothing about the CRAA scaffold (**1**) that would inherently preclude transport across cell walls. Of course, cell wall penetration will vary significantly depending on the bacteria in question and is based on what is attached to the CRAA (**1**) linker (as in Figure 1), but these results are encouraging in that at least in some cases cell wall penetration will be possible.

Next, to assess whether the CRAA scaffold (**1**) is a privileged scaffold for NAD(P)(H)-binding proteins and to identify potential target and antitarget proteins, crude cell lysates from *E. coli* and *M. tuberculosis* were both loaded onto the affinity column and proteins eluted using free CRAA (**1**) probe (Figure 5). SDS−PAGE analysis of both microbial samples showed very similar patterns (Figure 6a), suggesting some overlap in their dehydrogenase subproteomes and corresponding binding profiles for the CRAA privileged scaffold (**1**), although some of this apparent overlap may also be due to the prevalence of proteins in this molecular weight range. Because *Mycobacterium tuberculosis* is of greater interest as a drug target,[40,41] proteomics studies were pursued to identify potential targets in its proteome. Interestingly, 4 out of the top 6 scoring proteins from the *Mycobacterium tuberculosis* proteome were NAD(P)(H)-binding proteins, although this was not obvious based on the initial annotation of the database (3 out of the 4 hits were for proteins of undefined function). An analogous study with a human liver proteome sample also resulted in the identification of proteins that were mostly (>50%) NAD(P)(H)-binding proteins. Given that most proteomes comprise <5% dehydrogenases,[23] the CRAA scaffold (**1**) appears to have good selectivity for this gene family. Now, any proteins that were identified in either the human or *Mycobacterium tuberculosis* proteomes have a baseline affinity for **1**, so more potent inhibitors could easily be made for a target of interest using the biligand design strategy outlined in Figure 1 and previously validated.[21] Only pursuing protein targets for which the start of a potent inhibitor/drug lead is available is highly pragmatic because it identifies "druggable" targets at the start of the drug discovery process. But are any of the identified proteins in Tables 1 and 2 drug targets, and/or are they worth pursuing as targets of chemical genetic probes for basic research objectives (i.e., functional genomics)?

Any drug designed to be an anti-infective would need to be optimized to not disrupt function of vital proteins in the human proteome. And since the liver is the body's first line of defense (after passage through the intestinal mucosa) before drugs go into the general circulation, proteome profiling was done against the human liver proteome. Of the human liver proteins identified (Table 1), 5 out of 6 (excluding keratin) were dehydrogenases. In terms of antitargets of concern, any drug leads designed using the CRAA (**1**) privileged scaffold (Figure 1) should certainly be tested against malate, glutamate, isocitrate, and the various aldehyde dehydrogenases listed in Table 1 and in Supporting Information. It is also noted that some of these proteins may prove to be useful targets for human disease in their own right. In this regard, it is interesting that CRAA (**1**) has affinity for various aldehyde dehydrogenases. This is perhaps not surprising because the drug epalrestat, also known as ONO-2235,[27,28] also contains a rhodanine core and is an aldose reductase inhibitor used to treat diabetes. Indeed, this suggests that our CRAA core (**1**) might be used as a starting point for building other aldose reductase inhibitors, with different and tunable off-target binding profiles. Another human enzyme that may bind **1** is NADP-dependent leukotriene B4 12-hydroxydehydrogenase, which is involved in eicosanoid inactivation and is a target of indomethacin[42] as well as other nonsteroidal anti-inflammatory drugs (NSAIDs).[43] Our proteome fishing data suggest that **1** might also be pursued as a starting point for inhibitors of this enzyme by properly tuning affinity based on what fragments are added to the scaffold (Figure 1). Another enzyme that may bind **1** is α-aminoadipic semialdehyde dehydrogenase (AASD). Genetic deficiency in AASD is known to cause pyridoxine-dependent epilepsy.[44,45] While seizures in such individuals cannot be prevented using antiepileptic drugs, they can be avoided by treatment with pyridoxine.[46] So it appears that AASD is an antitarget to be avoided. But any potential problems from transient inhibition of AASD are likely to be less severe than the genetic knockout just described and in any case could be alleviated by treatment with pyridoxine. Conversely, the CRAA scaffold (**1**) could be used as a starting point for designing a more potent inhibitor of AASD (Figure 1) for chemical genetic studies in model organisms that contain close homologues of human AASD, such as zebrafish (gi27882244), rat (gi149064286), and *Xenopus* (gi51703516).

If any human proteins are to be pursued as drug targets, specificity should be checked against the other metabolically important dehydrogenases listed in Table 1 to avoid toxicity and to achieve an acceptable therapeutic index. So important outcomes of the human proteome data are (a) a list of targets that could be pursued in subsequent drug discovery efforts, especially for diabetes (aldose reducatse) and inflammation (NADP-dependent leukotriene B4 12-hydroxydehydrogenase), (b) a list of human antitargets for these drug discovery efforts, and (c) a proteomics-based strategy for assessing binding profiles (described in Figure 5) to assess off-target effects. Finally, these data confirm that **1** is behaving as a privileged scaffold for dehydrogenases, in the context of the human liver proteome.

Toward the goal of using the CRAA privileged scaffold (**1**) in anti-infective drug discovery efforts, analogous proteome fishing studies were performed using crude cell lysates from *Mycobacterium tuberculosis*. As with the human liver proteins, *M. tuberculosis* proteins were bound to the CRAA-affinity resin, then eluted with free **1**, and fractions were analyzed using tandem MS. Of the highest scoring *M. tuberculosis* proteins (score >13, Table 2), there were four possible pyridine nucleotide-binding proteins out of six proteins identified. Interestingly, three of the captured proteins had no annotated function, but subsequent NCBI searches and BLAST alignments identified the closest homologues to be NAD(P)(H)-binding proteins; this highlights the value of CRAA-based proteome fishing in functional proteomic efforts, even providing the start of a chemical genetic probe to later explore function. There is also some likelihood that one or more of these proteins could be drug targets. For example, the top scoring protein in Table 2 has high homology to a coenzyme F420-dependent N5,N10-methylene tetrahydromethanopterin reductase. Coenzyme F420 was first discovered in methanogenic archaea[47,48] and is now known to be present in mycobacteria. Indeed, Daniels has suggested that targeting of F420-dependent enzymes might be pursued as a new strategy for killing mycobacteria.[49] RibD, another *Mycobacterium tuberculosis* hit (Table 2), is essential for synthesis of riboflavin. While this may not be a viable drug target, a potent inhibitor of RibD would provide a chemical knockout to complement genetic knockouts of RibD (such mutants are riboflavin auxotrophs[50]), to explore function. One potential application might be to create transient vitamin B2 auxotrophy if one wanted to incorporate isotopically labeled riboflavin into a microbially expressed protein. Finally, the two "putative uncharacterized proteins" in Table 2 are also of interest not just as potential drug targets but because chemical genetic probes might help to better define their function. One of these proteins has the highest homology to 17-β-hydroxysteroid dehydrogenase/hydratase-dehydrogenase-epimerase, but very little is known about the role of 17-β-ketodehydrogenases in microbes. The human homologue (17-β-hydroxysteroid dehydrogenase) is involved in the synthesis of estradiol from estrone and so is a target for breast cancer and endometriosis.[51] What

metabolic role the microbial enzyme plays, and whether it is a viable drug target, is not known[52] but could certainly be probed with chemical genetic probes based on the CRAA scaffold (**1**). The other uncharacterized protein identified in Table 2 is in the nitroreductase family. Purkayastha et al.[53] have noted that nitroreductases may play a role in helping mycobacteria respond to different host conditions; for example, a nitroreductase is up-regulated when mycobacteria are inside the macrophage. Because mycobacteria survive and multiply inside macrophages,[54] it is important to better understand the enzymes that are up-regulated and perhaps facilitate their survival in this environment. Dissecting this regulatory regulatory cascade might uncover new drug targets and could possibly provide a better basic understanding of how the bacteria can hide within the host's own defense system. Higher affinity ligands constructed off the CRAA scaffold (**1**) would minimally serve as chemical genetic probes and perhaps even as drug leads.

Of the scaffold-binding *M. tuberculosis* proteins identified, it is certainly not yet known which (if any) will be useful drug targets because of a lack of proper annotation. But the above discussion points out an especially useful feature of the CRAA probe (**1**): it can be used both as a platform for drug design and for development of chemical genetic probes. That is, biligands designed with specificity for these proteins of unknown function could then be used to explore phenotypic effects of a chemical knockout. If the phenotypic effect suggests a mechanism to kill the microbe, then at least there is the start a drug lead in hand. The intention of this study, then, is to prepare a foundation for future drug design and chemical genetic initiatives by providing a chemical scaffold for optimization (CRAA, **1**), a strategy for using it to generate new and potent biligand inhibitors (Figure 1), a proteome-wide method for assessing target and antitarget binding broadly (Figures 5 and 6) to correlate with phenotypic effects, and a list of targets and antitargets in both human and *Mycobacterium tuberculosis* to begin pursuing (Tables 1–3).

Methods

Equipment and Materials. Nano-HPLC-mass spectrometry was performed using an LTQ mass spectrometer (Thermo-Fisher) coupled to a Surveyor HPLC system (Thermo Fisher) equipped with a Finnigan Micro AS autosampler. The instrument was interfaced with an Aquasil C18 PicoFrit capillary column (75 μm $\times$ 10 cm) from New Objective. A Kodak Image Station 2000MM System was used for gel fluorescence scanning (Figure 3b), and an Olympus BX60 microscope was used for fluorescene imaging of cells (Figure 4). All Novex gel products for the SDS−PAGE experiments were from Invitrogen, as was the SilverQuest staining kit. All salts, buffers, enzymes, and other chemical reagents are from Sigma-Aldrich and are of biochemical reagent grade, unless specified otherwise. The ω-aminohexylagarose and the human liver proteins (cytoplasmic) are also from Sigma. The *M. tuberculosis* H37Rv whole cell lysate was from Colorado State University. These proteins are from cells that were grown in glycerol−alanine stocks for 14 days, then washed with PBS. After γ-irradiation (to inactivate), cells were disrupted (French Press) and the lysate was centrifuged to remove cell debris. Lysis buffer was PBS with 8 mM EDTA and protease inhibitors. Further details are available at www.cvmbs.colostate.edu/microbiology/tb/cellysate.htm.

Synthesis of 1 (CRAA): 5-[(3,4-Dihydroxyphenyl)methylene]-4-oxo-2-thioxo-3-thiazolidineacetic Acid. Synthesis was largely as described before.[37] Briefly, 3-rhodanine acetic acid was reacted with 3,4-dihydroxybenzaldehyde in acetic acid/acetate at 90 °C for 6 h. After the mixture was cooled, yellow crystals were poured into cold water, filtered, washed, and then crystallized from acetic acid.

Synthesis of 2 (NHS-CRAA): (5-[(3,4-Dihydroxyphenyl)-methylene]-4-oxo-2-thioxo-3-thiazolidineacetic *N*-Hydroxysuccinimide Ester).[55] Under a N_2 atmosphere, a mixture of 6.22 g of **1**, 5.75 g of *N*-hydroxysuccinimide, 20.6 g of DCC, 50 mL of DMSO, and a small amount of DMAP catalyst was reacted at room temperature overnight. The next day the reaction was monitored by NMR (Supporting Information Figure S6) and with TLC (using EMD silica gel 60 F_{254} developed with chloroform/methanol/acetic acid, 12:3:1 v/v/v), visualized using a 254 nm UV light (the R_f of **1** is 0.39 and the new spot's R_f is 0.68). The DCU (dicyclohexylureo) was vacuum-filtered off, and the NHS-CRAA (**2**, Figure 2) DMSO solution was used in the next step without further purification.

Synthesis of CRAA (1) Agarose Matrix (5-[(3,4-Dihydroxyphenyl)methylene]-4-oxo-2-thioxo-3-thiazolidineacetic ω-Aminohexylagarose Amide).[56] NHS-CRAA ester (**2**) DMSO solution was added dropwise into 100 mL of ω-aminohexylagarose suspended in 600 mL of 100 mM phosphate buffer, pH 10.0. During this process, the pH was maintained at 10.0, and then the reaction was run at 7 °C in a refrigerator overnight. The next day, 60 mL of 1 M Tris-HCl buffer, pH 6.5, was added to the reaction mixture to stop the reaction. Then 47.7 g of sodium chloride was added to form a final 0.5 M saline solution. The liquid layer was decanted, and the labeled matrix (Figure 2) was washed with a large amount of deionized water. Then ~10 mL of matrix was packed into a 1 cm $\times$ 20 cm column for column chromatography.

NHS-CRAA Ester (1) in In-Cell Uptake and Labeling Study.[57] *E. coli* containing the pET11a DHPR expression construct was inoculated into 30 mL of LB culture medium, growing overnight at 37 °C, 225 rpm. The next day, 10 mL of this culture was added to two flasks (flasks A and B, each containing 800 mL of LB medium with 50 μg/mL carbenicillin). The OD_{600} was monitored until it reached ~1.0. To flask A was added 0.8 mL of a 0.4 M IPTG stock to start induction.[58] Flask B was used as a control without induction. Five hours later, cells were collected (centrifuged 10 min at 4000 rpm) and washed once with 100 mM PBS buffer, pH 7.4. The cells were then suspended in 100 mL of pH 7.4 PBS buffer (8 g of NaCl, 0.2 g of KCl, 1.44 g of Na_2HPO_4, 0.24 g of KH_2PO_4 in 1.0 L) and incubated for 5 min. Then 1 mL of NHS-CRAA ester (**2**) was added to each flask and incubated at room temperature for about 30 min (Figure 3a). An amount of 10 mL of 1 M Tris-HCl, pH 6.5, was added to each flask and shaken for another 5 min to quench the reaction. The cells were collected again by centrifuging and washed twice with PBS buffer. The cells were lysed with SDS loading buffer (50 mM Tris-HCl (pH 6.8), 100 mM dithiothreitol, 2% SDS, 0.1% bromophenol blue, 10% glycerol) and were run on a 4−12% Bis-Tris SDS−PAGE gel (Figure 3b). The gel was fluorescently imaged on a Kodak Image Station to selectively detect **1** which has λ_{max} for absorbance and emission at 465 and 535 nm.[37] Cells were fluorescently imaged in PBS buffer after the wash (before lysis) using 495 nm/520 nm excitation/emission filters on the fluorescence microscope. Complementary fluorescence and bright field images may be shifted slightly relative to each other because of bacterial motion between image captures. Exposure time was 1/3.5 s, and 1000$\times$ magnification was used (Figure 4). Fluorescence images of control cells (no IPTG treatment, no DHPR) indicate much less labeling of cells, with the majority of the fluorescence coming from cellular debris (Supporting Information Figure S3).

General Procedure for CRAA (1) Affinity Column Chromatography and Target Fishing.[32] The CRAA (**1**) affinity column was equilibrated with buffer A, which contains 25 mM Tris-HCl, 50 mM NaCl, and 0.1% NaN_3, pH 7.8. Washing was done until the eluent was nearly colorless (**1** is intensely colored). Then the protein sample (*E. coli*, *M. tuberculosis* or human liver) was loaded onto the affinity column and washed with a large amount of buffer A until no protein sample was detected using a Bradford assay (BioRad). The buffer volume used was usually 10-fold of the packing volume of the column. Then the affinity column was eluted with buffer B, which is the same as buffer A except containing 4 mM **1**. Fractions were collected, then separated on an SDS−PAGE gel and stained using a SilverQuest kit. Fractions from *E. coli* and *M. tuberculosis* were compared and showed very similar banding

profiles based on SDS−PAGE gel analysis (Figure 6a). Human liver and *M. tuberculosis* fractions either were used directly for mass spectral analysis (next section) or were separated using SDS−PAGE, with protein extracted from the bands indicated in Figure 6c.

Sample Preparation for Mass Spectrometry. Pooled fractions, after elution from the CRAA (**1**) affinity column, were concentrated using a Centricon filter with 10 kDa cutoff (Millipore). Then 100 μL of affinity purified protein mixtures were polymerized in the presence of 100 μL of acrylamide/bis (30% T/2.67% C), 2 μL of 10% ammonium persulfate, and 2 μL of TEMED. With this mixture a 15% gel piece was formed. Polymerization was performed in the cap of an Eppendorf tube. The polymerized gel pieces were then transferred to the corresponding Eppendorf tube in 1 mL of 40% methanol and 7% acetic acid and incubated for 30 min. The gel pieces were washed twice in water for 30 min each time while sonicating. Gel pieces were then washed twice in 50% acetonitrile for 30 min each time while sonicating. The gel pieces were then washed twice again, this time in 50% acetonitrile in 50 mM ammonium bicarbonate, pH 8.0. The gel pieces were then dried using a speed vac from Savant. To each gel piece was added 200 μL of 20 mM ammonium bicarbonate, pH 8.0, containing 1 μg of trypsin (Promega); this was incubated overnight at 37 °C. Each gel piece with the digested proteins was then extracted twice with 70% acetonitrile in 0.1% formic acid. *From this step onward, all water used was MS quality water.* Corresponding extracts of each gel were pooled together and dried. To each dried sample was added 6 M guanidine·HCl in 5 mM potassium phosphate and 1 mM DTT, pH 6.5. This was sonicated, and peptides were extracted using a C_{18} ZipTip from Millipore. Extracted peptides were then collected into an insert in a vial to be used for mass spectrometry and dried in the inserts. To each dried sample was added 5 μL of 0.1% formic acid in MS water containing 5% acetonitrile. Samples were then ready for mass spectrometry and were injected into the LTQ LC/MS. The MS/MS data were collected and searched against the appropriate subset of the Uniprot database.

Acknowledgment. We thank Dr. John Blanchard (Albert Einstein College of Medicine, NY) for the DHPR (dapB) expression constructs, and Dr. M. Behnam Ghasemzadeh for use of the KODAK Image Station at the College of Health Sciences of Marquette University. *M. tuberculosis* H37Rv whole cell lysate was received as part of the National Institutes of Health and National Institute of Allergy and Infectious Disease Contract HHSN266200400091C, entitled Tuberculosis Vaccine Testing and Research Materials, which was awarded to the Colorado State University. Fluorescence microscopy was performed at the Children's Environmental Health Sciences Core (EHSC) Center, with expert assistance of Dr. Henry Tomasiewicz. The EHSC is supported in part by NIH Grant ES-04184.

Supporting Information Available: Additional gels, NMR characterization, and tables of mass spectral analyses. This material is available free of charge via the Internet at http://pubs.acs.org.

References

(1) Fitzgerald, G. A. Opinion: anticipating change in drug development: the emerging era of translational medicine and therapeutics. *Nat. Rev. Drug Discovery* **2005**, *4*, 815–818.
(2) Tolliday, N.; Clemons, P. A.; Ferraiolo, P.; Koehler, A. N.; Lewis, T. A.; Li, X.; Schreiber, S. L.; Gerhard, D. S.; Eliasof, S. Small molecules, big players: the National Cancer Institute's Initiative for Chemical Genetics. *Cancer Res.* **2006**, *66*, 8935–8942.
(3) Strausberg, R. L.; Schreiber, S. L. From knowing to controlling: a path from genomics to drugs using small molecule probes. *Science* **2003**, *300*, 294–295.
(4) Krishnamurty, R.; Maly, D. J. Chemical genomic and proteomic methods for determining kinase inhibitor selectivity. *Comb. Chem. High Throughput Screening* **2007**, *10*, 652–666.
(5) Daub, H.; Godl, K.; Brehmer, D.; Klebl, B.; Muller, G. Evaluation of kinase inhibitor selectivity by chemical proteomics. *Assay Drug Dev. Technol.* **2004**, *2*, 215–224.
(6) Peters, E. C.; Gray, N. S. Chemical proteomics identifies unanticipated targets of clinical kinase inhibitors. *ACS Chem. Biol.* **2007**, *2*, 661–664.
(7) Argyrou, A.; Jin, L.; Siconilfi.Baez, L.; Angeletti, R. H.; Blanchard, J. S. Proteome-wide profiling of isoniazid targets in *Mycobacterium tuberculosis*. *Biochemistry* **2006**, *45*, 13947–13953.
(8) Schalon, C.; Surgand, J. S.; Kellenberger, E.; Rognan, D. A simple and fuzzy method to align and compare druggable ligand-binding sites. *Proteins*, in press.
(9) Hajduk, P. J.; Huth, J. R.; Tse, C. Predicting protein druggability. *Drug Discovery Today* **2005**, *10*, 1675–1682.
(10) DeSimone, R. W.; Currie, K. S.; Mitchell, S. A.; Darrow, J. W.; Pippin, D. A. Privileged structures: applications in drug discovery. *Comb. Chem. High Throughput Screening* **2004**, *7*, 473–494.
(11) Duarte, C. D.; Barreiro, E. J.; Fraga, C. A. Privileged structures: a useful concept for the rational design of new lead drug candidates. *Mini-Rev. Med. Chem.* **2007**, *7*, 1108–1119.
(12) Costantino, L.; Barlocco, D. Privileged structures as leads in medicinal chemistry. *Curr. Med. Chem.* **2006**, *13*, 65–85.
(13) Muller, G. Medicinal chemistry of target family-directed masterkeys. *Drug Discovery Today* **2003**, *8*, 681–691.
(14) Bemis, G. W.; Murcko, M. A. The properties of known drugs. 1. Molecular frameworks. *J. Med. Chem.* **1996**, *39*, 2887–2893.
(15) Brustle, M.; Beck, B.; Schindler, T.; King, W.; Mitchell, T.; Clark, T. Descriptors, physical properties, and drug-likeness. *J. Med. Chem.* **2002**, *45*, 3345–3355.
(16) Peters, U.; Cherian, J.; Kim, J. H.; Kwok, B. H.; Kapoor, T. M. Probing cell-division phenotype space and Polo-like kinase function using small molecules. *Nat. Chem. Biol.* **2006**, *2*, 618–626.
(17) Smith, A. B., 3rd; Favor, D. A.; Sprengeler, P. A.; Guzman, M. C.; Carroll, P. J.; Furst, G. T.; Hirschmann, R. Molecular modeling, synthesis, and structures of N-methylated 3,5-linked pyrrolin-4-ones toward the creation of a privileged nonpeptide scaffold. *Bioorg. Med. Chem.* **1999**, *7*, 9–22.
(18) Amano, M.; Koh, Y.; Das, D.; Li, J.; Leschenko, S.; Wang, Y. F.; Boross, P. I.; Weber, I. T.; Ghosh, A. K.; Mitsuya, H. A novel bis-tetrahydrofuranylurethane-containing nonpeptidic protease inhibitor (PI), GRL-98065, is potent against multiple-PI-resistant human immunodeficiency virus in vitro. *Antimicrob. Agents Chemother.* **2007**, *51*, 2143–2155.
(19) Guo, T.; Hobbs, D. W. Privileged structure-based combinatorial libraries targeting G protein-coupled receptors. *Assay Drug Dev. Technol.* **2003**, *1*, 579–592.
(20) Sasse, B. C.; Mach, U. R.; Leppaenen, J.; Calmels, T.; Stark, H. Hybrid approach for the design of highly affine and selective dopamine D(3) receptor ligands using privileged scaffolds of biogenic amine GPCR ligands. *Bioorg. Med. Chem.* **2007**, *15*, 7258–7273.
(21) Sem, D. S.; Bertolaet, B.; Baker, B.; Chang, E.; Costache, A. D.; Coutts, S.; Dong, Q.; Hansen, M.; Hong, V.; Huang, X.; Jack, R. M.; Kho, R.; Lang, H.; Ma, C. T.; Meininger, D.; Pellecchia, M.; Pierre, F.; Villar, H.; Yu, L. Systems-based design of bi-ligand inhibitors of oxidoreductases: filling the chemical proteomic toolbox. *Chem. Biol.* **2004**, *11*, 185–194.
(22) Kho, R.; Newman, J. V.; Jack, R. M.; Villar, H. O.; Hansen, M. R. Genome-wide profile of oxidoreductases in viruses, prokaryotes, and eukaryotes. *J. Proteome Res.* **2003**, *2*, 626–632.
(23) Kho, R.; Baker, B. L.; Newman, J. V.; Jack, R. M.; Sem, D. S.; Villar, H. O.; Hansen, M. R. A path from primary protein sequence to ligand recognition. *Proteins* **2003**, *50*, 589–599.
(24) Godl, K.; Wissing, J.; Kurtenbach, A.; Habenberger, P.; Blencke, S.; Gutbrod, H.; Salassidis, K.; Stein-Gerlach, M.; Missio, A.; Cotten, M.; Daub, H. An efficient proteomics method to identify the cellular targets of protein kinase inhibitors. *Proc. Natl. Acad. Sci. U.S.A.* **2003**, *100*, 15434–15439.
(25) Bantscheff, M.; Eberhard, D.; Abraham, Y.; Bastuck, S.; Boesche, M.; Hobson, S.; Mathieson, T.; Perrin, J.; Raida, M.; Rau, C.; Reader, V.; Sweetman, G.; Bauer, A.; Bouwmeester, T.; Hopf, C.; Kruse, U.; Neubauer, G.; Ramsden, N.; Rick, J.; Kuster, B.; Drewes, G. Quantitative chemical proteomics reveals mechanisms of action of clinical ABL kinase inhibitors. *Nat. Biotechnol.* **2007**, *25*, 1035–1044.
(26) Poupaert, J.; Carato, P.; Colacino, E.; Yous, S. 2(3*H*)-Benzoxazolone and bioisosters as "privileged scaffold" in the design of pharmacological probes. *Curr. Med. Chem.* **2005**, *12*, 877–885.
(27) Matsuoka, K.; Sakamoto, N.; Akanuma, Y.; Hotta, N.; Shichiri, M.; Toyota, T.; Oka, Y.; Kawamori, R.; Shigeta, Y. ADCT Study Group. A long-term effect of epalrestat on motor conduction velocity of diabetic patients: ARI-Diabetes Complication Trial. *Diabetes Res. Clin. Pract.* **2007**, *77*, S263−268.
(28) Hotta, N.; Akanuma, Y.; Kawamori, R.; Matsuoka, K.; Oka, Y.; Shichiri, M.; Toyota, T.; Nakashima, M.; Yoshimura, I.; Sakamoto, N.; Shigeta, Y. ADCT Study Group. Long-term clinical effects of epalrestat, an aldose reductase inhibitor, on diabetic peripheral neuropathy. *Diabetes Care* **2006**, *29*, 1538–1544.

(29) Bolton, J. L.; Pisha, E.; Shen, L.; Krol, E. S.; Iverson, S. L.; Huang, Z.; van.Breemen, R. B.; Pezzuto, J. M. The reactivity of *o*-quinones which do not isomerize to quinone methides correlates with alkylcatechol-induced toxicity in human melanoma cells. *Chem. Biol. Interact.* **1997**, *106*, 133–148.

(30) Hutzler, J. M.; Melton, R. J.; Rumsey, J. M.; Thompson, D. C.; Rock, D. A.; Wienkers, L. C. *Chem. Res. Toxicol.*, in press.

(31) Barry, S.; O'Carra, P. Affinity chromatography of nicotinamide−adenine dinucleotide-linked dehydrogenases on immobilized derivatives of the dinucleotide. *Biochem. J.* **1973**, *135*, 595–607.

(32) Morelli, A.; Benatti, U. Simple chemical synthesis of a specific effector for the affinity chromatography of nicotinamide adenine dinucleotide phosphate-dependent dehydrogenases. *Ital. J. Biochem.* **1974**, *23*, 279–291.

(33) Trayer, I. P.; Trayer, H. R. Affinity chromatography of nicotinamide nucleotide-dependent dehydrogenases on immobilized nucleotide derivatives. *Biochem. J.* **1974**, *141*, 775–787.

(34) Ng, E.; Schriemer, D. C. Emerging challenges in ligand discovery: new opportunities for chromatographic assay. *Expert Rev. Proteomics* **2005**, *2*, 891–900.

(35) Bertrand, R.; Derancourt, J.; Kassab, R. Fluorescence characterization of structural transitions at the strong actin binding motif in skeletal myosin affinity labeled at cysteine 540 with novel spectroscopic cysteaminyl mixed disulfides. *Biochemistry* **2000**, *39*, 14626–14637.

(36) Scapin, G.; Reddy, S. G.; Zheng, R.; Blanchard, J. S. Three-dimensional structure of *Escherichia coli* dihydrodipicolinate reductase in complex with NADH and the inhibitor 2,6-pyridinedicarboxylate. *Biochemistry* **1997**, *36*, 15081–15088.

(37) Ge, X.; Sem, D. S. Affinity-based chemical proteomic probe for dehydrogenases: fluorescence and visible binding assays in gels. *Anal. Biochem.* **2007**, *370*, 171–179.

(38) Barglow, K. T.; Cravatt, B. F. Activity-based protein profiling for the functional annotation of enzymes. *Nat. Methods* **2007**, *4*, 822–827.

(39) Evans, M. J.; Saghatelian, A.; Sorensen, E. J.; Cravatt, B. F. Target discovery in small-molecule cell-based screens by in situ proteome reactivity profiling. *Nat. Biotechnol.* **2005**, *23*, 1303–1307.

(40) Dye, C.; Scheele, S.; Dolin, P.; Pathania, V.; Raviglione, M. C. Consensus statement. Global burden of tuberculosis: estimated incidence, prevalence, and mortality by country. WHO Global Surveillance and Monitoring Project. *JAMA, J. Am. Med. Assoc.* **1999**, *282*, 677–686.

(41) Okada, M.; Kobayashi, K. Recent progress in mycobacteriology. *Kekkaku* **2007**, *82*, 783–799.

(42) Hori, T.; Ishijima, J.; Yokomizo, T.; Ago, H.; Shimizu, T.; Miyano, M. Crystal structure of anti-configuration of indomethacin and leukotriene B4 12-hydroxydehydrogenase/15-oxo-prostaglandin 13-reductase complex reveals the structural basis of broad spectrum indomethacin efficacy. *J. Biochem.* **2006**, *140*, 457–466.

(43) Clish, C. B.; Sun, Y. P.; Serhan, C. N. Identification of dual cyclooxygenase−eicosanoid oxidoreductase inhibitors: NSAIDs that inhibit PG-LX reductase/LTB(4) dehydrogenase. *Biochem. Biophys. Res. Commun.* **2001**, *288*, 868–874.

(44) Mills, P. B.; Struys, E.; Jakobs, C.; Plecko, B.; Baxter, P.; Baumgartner, M.; Willemsen, M. A.; Omran, H.; Tacke, U.; Uhlenberg, B.; Weschke, B.; Clayton, P. T. Mutations in antiquitin in individuals with pyridoxine-dependent seizures. *Nat. Med.* **2006**, *12*, 307–309.

(45) Bok, L. A.; Struys, E.; Willemsen, M. A.; Been, J. V.; Jakobs, C. Pyridoxine-dependent seizures in Dutch patients: diagnosis by elevated urinary alpha-aminoadipic semialdehyde levels. *Arch. Dis. Child.* **2007**, *92*, 687–689.

(46) Salomons, G. S.; Bok, L. A.; Struys, E. A.; Pope, L. L.; Darmin, P. S.; Mills, P. B.; Clayton, P. T.; Willemsen, M. A.; Jakobs, C. An intriguing "silent" mutation and a founder effect in antiquitin (ALDH7A1). *Ann. Neurol.* **2007**, *62*, 414–418.

(47) Eirich, L. D.; Vogels, G. D.; Wolfe, R. S. Distribution of coenzyme F420 and properties of its hydrolytic fragments. *J. Bacteriol.* **1979**, *140*, 20–27.

(48) Eirich, L. D.; Vogels, G. D.; Wolfe, R. S. Proposed structure for coenzyme F420 from Methanobacterium. *Biochemistry* **1978**, *17*, 4583–4593.

(49) Purwantini, E.; Daniels, L. Molecular analysis of the gene encoding F420-dependent glucose-6-phosphate dehydrogenase from *Mycobacterium smegmatis*. *J. Bacteriol.* **1998**, *180*, 2212–2219.

(50) Salvetti, S.; Celandroni, F.; Ghelardi, E.; Baggiani, A.; Senesi, S. Rapid determination of vitamin B2 secretion by bacteria growing on solid media. *J. Appl. Microbiol.* **2003**, *95*, 1255–1260.

(51) Messinger, J.; Hirvela, L.; Husen, B.; Kangas, L.; Koskimies, P.; Pentikainen, O.; Saarenketo, P.; Thole, H. New inhibitors of 17beta-hydroxysteroid dehydrogenase type 1. *Mol. Cell. Endocrinol.* **2006**, *248*, 192–198.

(52) Rizner, T. L.; Zakelj-Mavric, M. Characterization of fungal 17beta-hydroxysteroid dehydrogenases. *Comp. Biochem. Physiol., Part B: Biochem. Mol. Biol.* **2000**, *127*, 53–63.

(53) Purkayastha, A.; McCue, L. A.; McDonough, K. A. Identification of a *Mycobacterium tuberculosis* putative classical nitroreductase gene whose expression is coregulated with that of the acr gene within macrophages, in standing versus shaking cultures, and under low oxygen conditions. *Infect. Immun.* **2002**, *70*, 1518–1529.

(54) Srivastava, V.; Rouanet, C.; Srivastava, R.; Ramalingam, B.; Locht, C.; Srivastava, B. S. Macrophage-specific *Mycobacterium tuberculosis* genes: identification by green fluorescent protein and kanamycin resistance selection. *Microbiology* **2007**, *153*, 659–666.

(55) Vanin, E. F.; Ji, T. H. Synthesis and application of cleavable photoactivable heterobifunctional reagents. *Biochemistry* **1981**, *20*, 6754–6760.

(56) Witzemann, V.; Muchmore, D.; Raftery, M. A. Affinity-directed cross-linking of membrane-bound acetylcholine receptor polypeptides with photolabile alpha-bungarotoxin derivatives. *Biochemistry* **1979**, *18*, 5511–5518.

(57) Waugh, S. M.; DiBella, E. E.; Pilch, P. F. Isolation of a proteolytically derived domain of the insulin receptor containing the major site of cross-linking/binding. *Biochemistry* **1989**, *28*, 3448–3455.

(58) Reddy, S. G.; Sacchettini, J. C.; Blanchard, J. S. Expression, purification, and characterization of *Escherichia coli* dihydrodipicolinate reductase. *Biochemistry* **1995**, *34*, 3492–3501.

JM8002284